

## Effect of Amine Ligands on Stabilization of Pt Nanoparticles as Electrode Materials for Electro-oxidation of Methanol

M.A. Dominguez-Crespo<sup>1,\*</sup>, E. Ramirez-Meneses<sup>1</sup>, A.M. Torres-Huerta<sup>1</sup> and H. Dorantes-Rosales<sup>2</sup>

<sup>1</sup>Instituto Politécnico Nacional, Grupo de Ingeniería en Procesamiento de Materiales CICATA-IPN, Unidad Altamira,  
km 14.5, Carretera Tampico-Puerto Industrial Altamira. C. P. 89600. Altamira, Tamps. MÉXICO.

<sup>2</sup>Instituto Politécnico Nacional, Departamento de Metalurgia, Escuela Superior de Ingeniería Química e Industrias Extractivas-IPN,  
C. P. 07300. D.F. MÉXICO.

Received: November 26, 2009, Accepted: December 09, 2010, Available online: January 07, 2011

**Abstract:** Pt-stabilized catalysts with platinum crystallites sizes between 1-20 nm were prepared using an organometallic approach and three different amino ligands; tert-butylamine, 1,3-diaminopropane and anthranilic acid. The electrochemical oxidation of methanol was investigated on Pt stabilized nanoparticles in acid solutions and the results were compared with commercial Pt<sub>Black</sub> to analyze the feasibility of applying a tailored stabilizer to improve the dispersion and electrocatalytic activity. The particle size and the degree of dispersion of the resultant nanoparticles were observed by transmission electron microscopy (TEM) and selected area electron diffraction (SAED) patterns. Dispersion differences, lattice parameters and interplanar distances were caused by the coordination of the functional groups contained in the ligands at the Pt surface. The current density peaks on methanol oxidation reaction (MOR), appearing at different potentials and are increased in the following order Pt<sub>Black</sub> ≈ Pt<sub>TBA</sub> > Pt<sub>DAP</sub> > Pt<sub>AA</sub>. The different tendency to form aggregates and scattered particles is the result of the divergence in their sterical shapes rather than different acid-base interactions. It has been also found that stabilized Pt nanoparticles using TBA or even DAP exhibit an interesting electrocatalytic activity, and can facilitate the MOR.

**Keywords:** Pt nanoparticles, methanol oxidation reaction, amine ligands, cyclic voltammetry, ac impedance.

### 1. INTRODUCTION

Synthesis and chemical and physical properties of metal nanoparticles (NPs) are currently of considerable interest because of their potential applications in materials science. This attention in the properties of these nano-objects has given rise to the need for the control of size, shape and monodispersity of the nanoparticles. It was recently demonstrated that the decomposition of organometallic precursors in the presence of H<sub>2</sub> or CO could reproducibly lead in certain cases to metal NPs displaying a very narrow size distribution [1]. Chaudret and co-workers [2-7] have developed an organometallic approach to the synthesis of noble metal nanoparticles by mild conditions to decompose metal complexes under dihydrogen. This method is suitable for obtaining monodispersed particles of very small size (1-2 nm) and performing coordination chemistry on their surface. Therefore, the use of organometallic precursors is now a well-established method for

obtaining both controlled size and surface state nanoparticles under mild conditions (room temperature and 1-3 bar of a reactive gas). As far as metallic nanoparticles are concerned, the common methods to stabilize the nanoparticles and control their growth is to use polymers [2,8,9] or ligands. These ligands may be relatively traditional (thiols [10-12], amines [6, 13, 14], phosphines [15-17], phenantroline [18, 19]) or more unusual such as the polyoxo anions used by Finke and coworkers [20, 21] or the fluorous ligands employed by Moreno-Mañas et al. [22, 23]. However, while it is well-known that the ligands will be determinant for inducing a specific reactivity to molecular complexes, little is known on the role of the ligands when coordinated to the surface of nanoparticles and their effect on different catalytic reactions. In order to gain high performance materials, it is of paramount importance that nanoparticle size and structure have to be controlled and it is believed [2, 6, 13, 24-30] that low precursor concentration and the presence of stabilizing agents are necessary to obtain NPs of controlled size. On the other hand, the proton exchange membrane fuel cell (PEMFC) is a highly attractive power source for mobile

\*To whom correspondence should be addressed: Email: mdominguezc@ipn.mx,  
adcrespo2000@yahoo.com.mx

and stationary applications due to its high power density at lower temperatures (55–95 °C) and its compact design. A large amount of work has been devoted to reduce the material costs of PEMFCs to achieve their widespread application, including the method of preparing a Pt catalyst with a large specific surface area to minimize the amount (and cost) of Pt required for a given level of activity [31, 32]. In spite of the advantages shown by DMFCs, potentially high energy content per unit mass and environmental friendliness that surpasses any petroleum product, methanol (as a fuel) has displayed poor electrochemical reactivity in acid solutions, except at high electrode potentials. Therefore, a catalyst is required to activate the reaction [33].

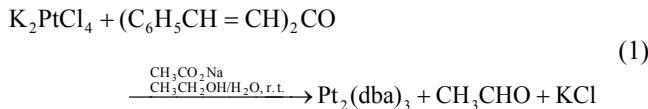
Industrial catalysts used in fuel cells are dominantly made of Pt nanoparticles [34]. Platinum has the highest catalytic activity for methanol oxidation in acid solutions, but the activity and long stability of both platinum and platinum black electrodes are too low for practical considerations. For this purpose, a large amount of work has been devoted to reduce the material costs of DMFCs to achieve their widespread application, including the method of preparing Pt and Pt-Metal catalysts with a large specific surface area to minimize the amount (and cost) of Pt required for a given level of activity [35, 36].

In previous work has been evidenced that the presence of donor ligands such as amines does not obstruct electron transfer for the oxygen reduction reaction [37]. As a continuation of such studies, in the current work, it is examined the feasibility of this method to use stabilized Pt NPs as electrode materials in Methanol Oxidation Reaction (MOR) in sulfuric acid solution. The obtained results were compared with commercial Pt/C NPs. The size and shape of the resultant nanoparticles were characterized by Transmission Electron Microscopy (TEM). The electrocatalytic activity of the electrode materials was investigated by cyclic voltammetry (CV) and ac impedance. The electrochemical experiments were performed by the thin porous coating electrode technique, which has proved to be very useful to study and evaluate supported catalysts of the type used in this work [38].

## 2. EXPERIMENTAL

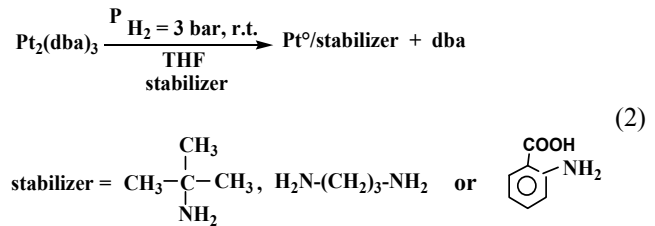
### 2.1. Synthesis and preparation of catalysts

The stabilized Pt catalysts, dispersed on vulcan carbon black, were obtained from the platinum precursor Tris (dibenzylideneacetone) diplatinum (0) or  $\text{Pt}_2(\text{dba})_3$ , which was prepared by using a procedure reported elsewhere [39] from  $\text{K}_2\text{PtCl}_4$  (Alfaesar, 99.9%). The synthesis of nanoparticles was carried out in a Fischer–Porter bottle at room temperature to obtain platinum colloids.



Three different compounds were employed to stabilize the platinum nanostructures; tert-butylamine, 1,3-diaminopropane and anthranilic acid using the following experimental procedure:  $\text{Pt}_2(\text{dba})_3$  (0.036 mmol) was introduced in a Fisher–Porter bottle under argon atmosphere and 40 mL of Tetrahydrofuran (THF) previously dis-

tilled and degassed by freeze-pump cycles. Thereafter, 0.6 mmol (10 eq.) of tert-butylamine (Aldrich, 98%) or 1, 3-diaminopropane (Aldrich, 99%) or anthranilic acid (Aldrich, 98%) was added to the resulting violet solution. Then, the obtained dark brown solutions were pressurized under dihydrogen atmosphere (3 bar) for 20 h. Afterwards, a homogeneous black colloidal solution was obtained. The colloidal solutions were purified by hexane washings (to eliminate the dibenzylideneacetone). Finally, the resulting black solution was evaporated in vacuum until the residue was completely dry. The one step synthesis of platinum nanoparticles was achieved according to following equation:



Diffuse reflectance-FTIR spectra were recorded on a Perkin–Elmer Spectrometer. GX (FT-IR) coupled with diffuse reflectance accessories. The samples have been prepared with a small quantity of each purified system and grounded with KBr (Aldrich, 99% IR grade) and pressed into a pellet. For the TEM analysis, a drop of each crude colloidal solution was deposited on a holey carbon coated copper grid. These analyses were performed on a JEOL-2000 FX II electron microscope, operating at 200 kV.

Glassy carbon discs were used as electrode supports. Before each experiment, the disc electrodes were mechanically polished by using emery paper, cloth and alumina powder (ca. 0.3 μm); and then electrochemically activated by pre-electrolysis. A suspension containing a 4:1 ratio of Vulcan carbon black / total metal (20 wt %) powders in deionized water was prepared, and the mixture was ultrasonicated for 30 min. Thereafter, the working electrode was prepared by attaching 3 μL of the solution onto the glassy carbon, and drying under a high purity argon flow at room temperature; the deposited catalyst layer was then covered with 4 μL of a diluted aqueous Nafion solution (ratio of Nafion/water solution 1:3). Finally, the electrode was immersed in a nitrogen purged electrolyte to record the electrochemical measurements.

### 2.2. Electrochemical measurements

Half-cell performance tests with a Luggine capillary were performed in a three electrode cell. A Pt grid and a saturated calomel electrode (SCE) were used as counter electrode and reference electrode, respectively. All the potentials in this paper are reported with respect to the standard hydrogen electrode (SHE). The electrolyte solution was prepared with deionized water Type I (18 MW) containing 0.5M  $\text{H}_2\text{SO}_4$  and 0.1M  $\text{CH}_3\text{OH}$ . The electrolytes were saturated with purified  $\text{N}_2$  gas. The electrochemical characterization of the catalysts was performed using cyclic voltammetry (CV) and electrochemical impedance spectroscopy (EIS) at room temperature in an AUTOLAB 30 potentiostat coupled to a personal computer. The cyclic voltammograms were adjusted in the interval ranging from -40 to 1450 mV vs. SHE at a scan rate of 20 mV s<sup>-1</sup> during 50 cyclic potentials scans. The charge of hydrogen oxidation can be obtained by integrating the CVs within the potential ranging from 0

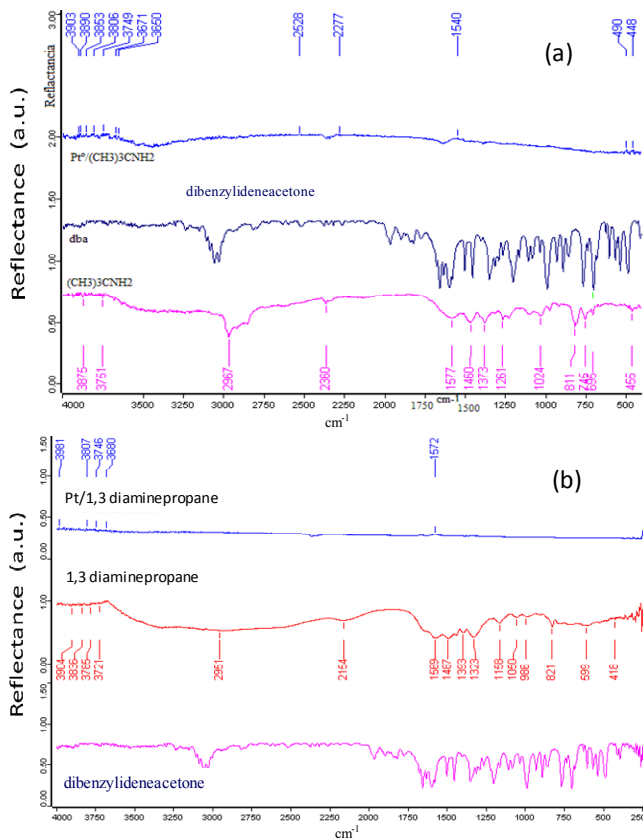


Figure 1. Diffuse reflectance-FTIR spectra recorded after the purification step of colloidal solutions (a)  $\text{Pt}/(\text{CH}_3)_3\text{CNH}_2$  and (b)  $\text{Pt}/1,3$  diaminepropane.

to 400 mV vs. SHE. This charge is representative of the electrochemically active surface area of the deposited platinum particles. The impedance of the working electrode in the methanol concentration was also measured. The impedance spectra were obtained at two different electrode potentials over methanol oxidation reaction (400, 900 mV). During the measurements, the frequency was varied from  $10^4$  to 0.01 Hz (ten frequency points per decade) with amplitude of the sinusoidal potential signal of 10 mV.

### 3. RESULTS AND DISCUSSION

#### 3.1. FT-IR spectroscopy

The diffuse reflectance spectra of  $\text{Pt}(\text{CH}_3)_3\text{CNH}_2$  and  $\text{Pt}/1,3$  diaminepropane particles synthesized in THF are shown in Figure 1a-b. For comparison also is showed the spectra for terbutyl amine,  $(\text{CH}_3)_3\text{CNH}_2$ , 1,3-diaminepropane and dibenzylideneacetone. The spectra recorded on purified colloids shows slightly bands at 3903–1540 corresponding to N–H and/or C–H stretching vibrations, thus confirming the presence of amine ligands near the surface of the particles. However, it cannot discard that some of these could be attributed to dba, arising from the Pt precursor, or to some of its derivatives. The tiny signals are due to the elimination of excessive stabilizer over metallic particles. In addition, it is well known that the stabilization depends upon the amount of amine and the solvent, i.e. the fast exchange between free and coordinated amines to

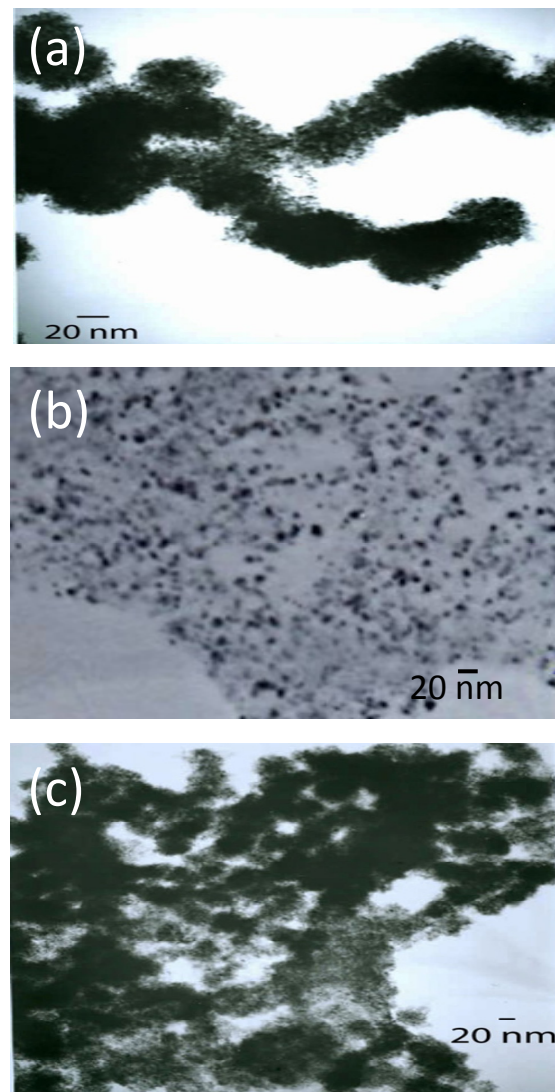


Figure 2. TEM micrographs and their corresponding selected area electron diffraction patterns of platinum nanoparticles stabilized by (a) tert-butylamine ( $\text{Pt}_{\text{TBA}}$ ), (b) 1,3-diaminopropane ( $\text{Pt}_{\text{DAP}}$ ) and (c) anthranilic acid ( $\text{Pt}_{\text{AA}}$ ).

the surface of Pt particles. The excess of amine groups was necessary to guarantee spherical nanoparticles.

#### 3.2. TEM analyses

Figure 2a-c shows typical transmission electron microscopic (TEM) images of Pt nanostructures stabilized by different amino ligands prepared by an organometallic approach. Comparing TEM images and particle size distributions, the Pt nanoparticles displayed secondary structures which are formed with primary semi-spherical particles. According to the histogram measured from an analysis of 200 particles in Figure 3; the 1,3-diaminepropane display the smallest particle size distribution ranging from 1 to 9 nm. Whereas, TBA and AA displayed particle size ranging from 6 to 18 nm and 8 to 20 nm, respectively. The corresponding selected area

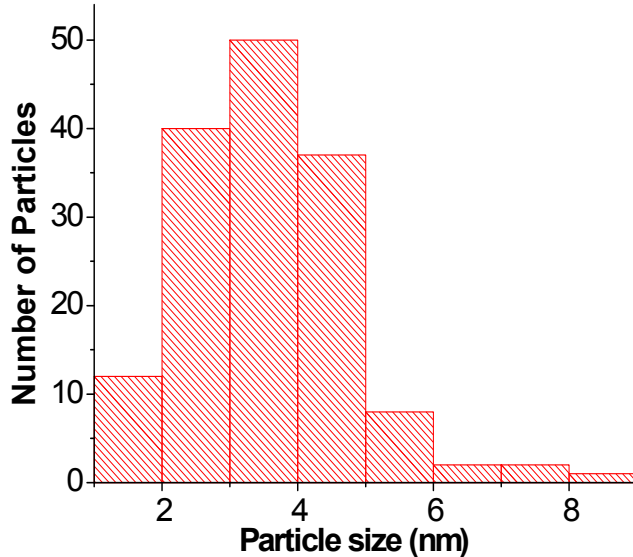


Figure 3. Particle size distribution histogram of stabilized Pt nanoparticles using DAP as ligand and measured from figure 2(b).

electron diffraction pattern (not shown here) confirms the presence of FCC platinum with interplanar distances and lattice parameters compared to those reported by JCPDS charts (04-0802), Table 1. It is noteworthy that the contributions of the ligands cause small discrepancies in the interatomic distances (below 0.03 Å). This effect has been previously suggested by Rodriguez et al., using CO ligands on the surface of Pt nanoparticles [25], who found that depending upon the ligands present in the coordination sphere, the structure can be changed; however, in our case, amines are considered as “weak” ligands and cannot provoke significant structural changes as in the case of bulky ligands (triphenylphosphine) or CO. This phenomenon could be explained as follows: The nature of the atom at the center and surface of the cluster is different. At the center, the atom is saturated by other atoms, but at the surface this is not the case. The atoms at the surface are coordinately unsaturated. That is why the capping agents, which are basically electron density donors, attached themselves at the surface of the nanocrystals, as is the case with the amino groups. In addition, the role of these ligands is well known due to metal colloids are inherently unstable with regard to aggregation, which eventually leads to pre-

Table 1. Lattice parameters and interplanar distances obtained from SAED of stabilized Pt nanoparticles.

Planes (h k l)	Pt <sub>TBA</sub>	Pt <sub>DAP</sub>	Pt <sub>AA</sub>	Pt <sub>theoretical</sub>
interplanar distances (Å)				
(111)	2.2818	2.2922	2.2818	2.2650
(200)	1.9763	1.9921	1.9764	1.9616
(220)	1.3716	1.4061	1.3905	1.3873
(311)	1.1839	1.1840	1.1896	1.1826
(331)	0.8996	0.8996	0.8884	0.9000
Lattice parameter, a (nm)	0.3926	0.3956	0.3934	0.3923

cipitation; however, capping these nanoparticles with a monolayer of judiciously selected molecules let to stabilize them not only with respect to aggregation but also against corrosive chemical reactions. At short interparticle distances, two particles are attracted to each other by van der Waals forces in the absence of repulsive forces. The stability of suspensions of tiny solid particles in a liquid medium is ensured by the repulsion between the particles [40]. The adsorption of stabilizing agents to nucleated nanocrystals lowers the free energy of the surface and, therefore, the reactivity of the particles. Then, the stabilizers provide a physical barrier that prevents the metal surfaces from contacting each other directly. They can also change the surface charge of a cluster and thus change its stability toward aggregation [41, 42]. The combination of the energetic stabilization of the metal surface by the surfactant, the consequences of charge-charge interactions, and the steric repulsion between particles prevent the system from forming aggregates [43-45].

Afterward, the observed differences between the ligands used in this work can be related to the free energy surface and to the “weak” character of amine groups. We have recently been interested in the preparation of noble metal nanoparticles to control the shape and surface state of the particles when different amounts of amine ligands are present in the reaction medium [46, 47]. In these works, it was demonstrated that the stabilization and shape depend on the amine amount in the reaction medium and the coordinated or non-coordinated solvent. While low concentration of stabilizers can produce regular and noodle-like particle shapes or not stabilized nanoparticles, 10 eq. of stabilizer containing amine groups produced “sponge-like” particles [47]. Then, the presence of different ligands in this work also results in the characteristic “sponge-like” for the stabilized nanostructures starting from TBA and AA but in the case of 1,3-diaminopropane the particles are fairly polydisperse in size and shape; the polydispersity in nanoparticle sizes prevents the formation of agglomerate organized Pt nanoparticle assemblies with long-range order. The obtained larger arrangement of nanoparticles (TBA and AA) grew at the expense of smaller ones via the Ostwald ripening process, where small nanoparticles dissolved and grew into larger crystals [48-50]. Consequently, the formation of uniform and well-shaped particles can be accounted for as a consequence of balance between stabilization and crystal growth in the solvent. TEM analysis shows that the skeleton and functional groups of the stabilizer can interact more or less with the surface of the particles and could favor their growth in a singular shape. Briefly, the phase transfer and stability of Pt nanostructures using with 1,3-DAP as stabilizer seems to be better than the others obtained with TBA and AA. Although, the small size of the primary particles obtained with TBA and AA suggests that the synthesized systems could have a proper performance in the direct methanol oxidation reaction as electrode materials as it has been previously demonstrated with the oxygen reduction reaction [37] where, it was found that the amino compounds used as stabilizers did not inhibit the catalytic activity of the electrodes, mainly due to the electron donation effect from the nitrogen atom to the nanoparticle surfaces [48]. Moreover, it is widely accepted that the nitrogen atom contained in the functional group of the stabilizers will not cause the poisoning of the Pt nanostructures during methanol oxidation [49].

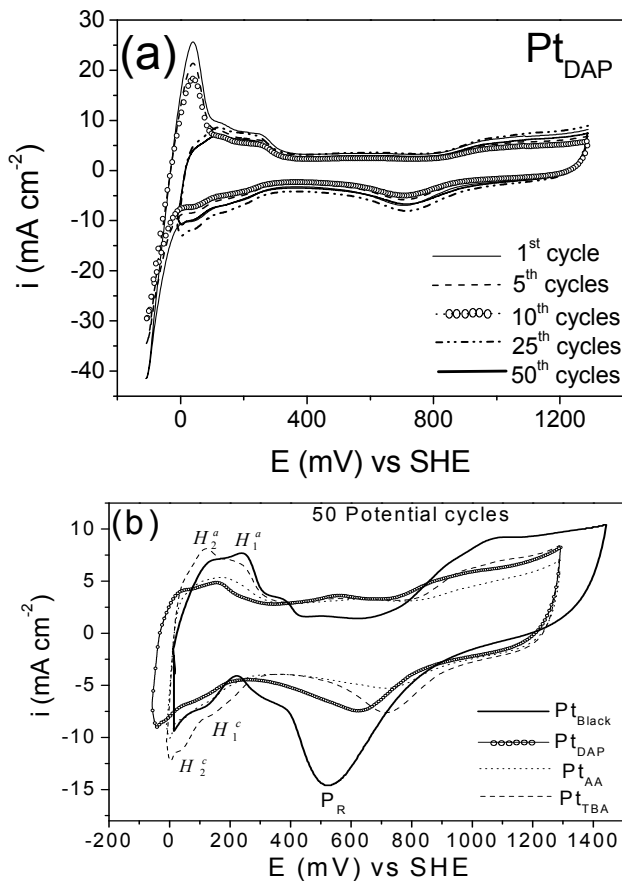


Figure 4. Cyclic voltammograms at  $20 \text{ mV s}^{-1}$  in  $0.5 \text{ M H}_2\text{SO}_4$  for stabilized Pt catalysts (a) Evolution with the potential cycles of  $\text{Pt}_{\text{DAP}}$  and (b) CVs of the different Pt catalysts after 50 potential cycles and their comparison with a commercial Pt catalysts.

### 3.3. Cyclic voltammetry studies

Figure 4a shows typical cyclic voltammetry curves obtained after one, five, ten, twenty- five and fifty potential sweeps for  $\text{Pt}_{\text{DAP}}$  nanoparticles in  $0.5 \text{ M H}_2\text{SO}_4$ . This figure highlights the surface stabilization, and after several potential cycles, the current density shows a significant reduction in the typical hydrogen desorption peaks on continuous potential cycling up to its stabilization after 25 potential cycles; although the tests were recorded up to 50 potential cycles to guarantee the chemical stability of the catalysts. The response of these peaks is also slightly shifted to positive potentials.

The dashed and solid lines with frame circles showed in Figure 4b are typical stabilized CV responses of different  $\text{Pt}_{\text{TBA}}$ ,  $\text{Pt}_{\text{DAP}}$  and  $\text{Pt}_{\text{AA}}$  catalysts at  $20 \text{ mV s}^{-1}$  in  $0.5 \text{ M H}_2\text{SO}_4$ . In order to observe the stabilizer influence, the positive limit was set below  $1450 \text{ mV}$  (SHE) and the negative at  $-40 \text{ mV}$ , before the oxygen and hydrogen evolution reactions were respectively, reached. The current densities are referred to the geometric area, which allows estimating if diffusion-limited electro-oxidation of bulk solution species is achieved.  $\text{Pt}_{\text{Black}}$  electrodes prepared from commercial ETEK nanoparticles with an average particle size in the range of 2-4 nm were also analyzed as a reference. In general, these CVs displayed

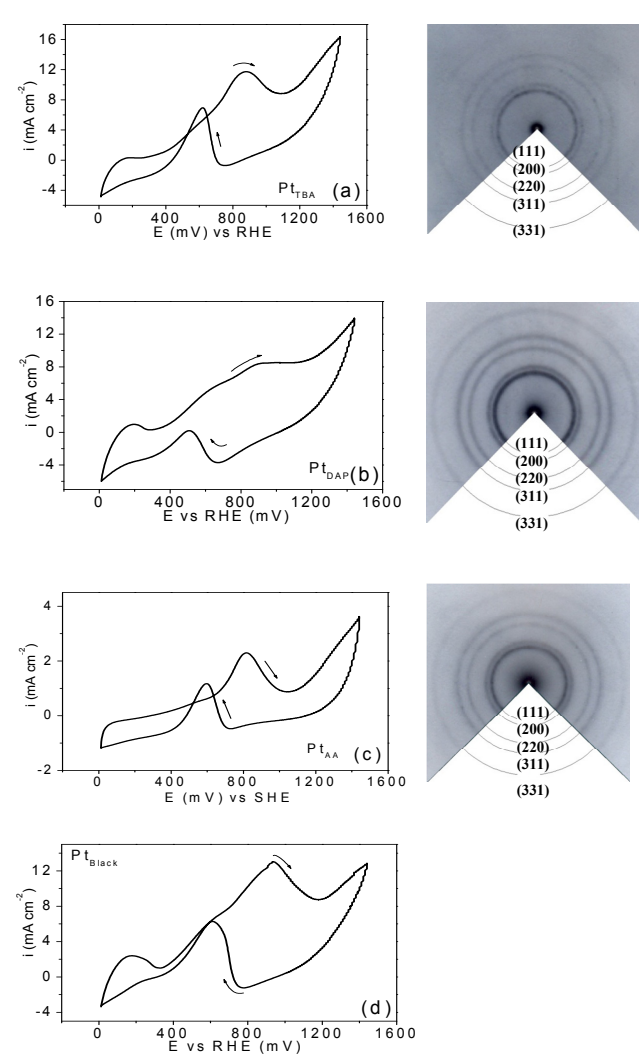


Figure 5. CV recorded of the stabilized Pt catalysts (and corresponding SAED patters) in a  $0.5 \text{ M H}_2\text{SO}_4 + 0.1 \text{ M CH}_3\text{OH}$  aqueous solution and argon atmosphere, after 50 potential cycles.

evidences of Pt electrode features. Although in some cases, the typical hydrogen adsorption( $\text{Pt-H}_{\text{ad}}$ )-desorption ( $\text{Pt-H}_{\text{des}}$ ) peaks of weakly and strongly adsorbed atoms are not well-resolved, in the potential range between 50 and  $400 \text{ mV}$  vs SHE, the peaks are related to the adsorption of hydrogen species. The observed voltammetric behavior of the stabilized catalysts was very similar in shape to that of the commercial  $\text{Pt}_{\text{Black}}$ ; however, the strong relationship of the hydrogen adsorption-desorption features with the nature of stabilizer is evident; i.e. two anodic (desorption) and cathodic (adsorption) peaks can be distinguishable for  $\text{Pt}_{\text{TBA}}$  and  $\text{Pt}_{\text{DAP}}$ , while in the stabilized Pt nanoparticles with anthranilic acid only one anodic peak is observed [49-51]. The so called “double layer region” is also observed in the potential range of  $400$ - $800 \text{ mV}$  followed by the oxide region where the formation of monolayer oxide begins at  $\sim 800 \text{ mV}$ . The capacitive current is slightly enhanced as a consequence of the presence of the stabilizer. This

effect was observed with the three electrodes; although for the TBA-stabilized Pt nanoparticles, this capacitive behavior is also accompanied by an improvement in the current density (shape of the CV profile). In this case, the  $\text{Pt}_{\text{TBA}}$  electrode is characterized by the following features: (i) Two adsorption-desorption hydrogen peaks, (ii) the hydrogen desorption continues over the double layer region even at potentials slightly higher than those observed for  $\text{Pt}_{\text{DAP}}$  and  $\text{Pt}_{\text{AA}}$  (iii) Pt-oxide formation occurs at a higher potential and oxide compounds are reduced at more positive potentials in comparison with  $\text{Pt}_{\text{Black}}$ . The evaluated electrodes follow the oxide formation on platinum according to the typical reactions [52]. The corresponding oxide reduction peak appears as a single cathodic peak, although it has been found that the reactions occur in two steps [53, 54].

In these reactions, the reversibility depends on the charge involved in the adsorption-desorption processes; therefore, it is clear that the behavior in the stabilized Pt electrodes is influenced by the nature of the stabilizer; in fact clear differences can be seen in the intensity and shape of the CVs when the stabilizer is present during the synthesis. From the results is evident that even the stabilized Pt particles showed higher particles size than that displayed by commercial  $\text{Pt}_{\text{Black}}$ , the behavior and surface area are comparable. The facts mentioned above suggest that the presence of suitable stabilizers on the nanoparticle surface modifies the dispersion, affecting their electrochemical behavior.

To compare the influence of the stabilizer nature on methanol tolerance, the CVs of the methanol oxidation reaction were carried out on the stabilized Pt nanostructures in nitrogen saturated 0.5 M  $\text{H}_2\text{SO}_4 + 0.1 \text{ M CH}_3\text{OH}$  solution and the plots are shown in Figure 5a-c. As a reference, the evolution of commercial  $\text{Pt}_{\text{Black}}$  is also shown (Figure 5d). The SAED patterns showed in Figures 5a-c on platinum nanoparticles prove that the order of magnitude of the mean diameter of metallic particles is still much smaller than 100 nm after the preparation of Pt catalysts. The voltammograms scanned in the presence of methanol impose remarkable charge imbalance and appear stretched, then in such conditions it is impossible directly to draw the zero current horizontal line. However, it is visible that all the three electrodes display some changes in the magnitude of current densities. In particular, among these Pt catalysts, the current density of the methanol oxidation on  $\text{Pt}_{\text{AA}}$  is much lower than that observed on  $\text{Pt}_{\text{TBA}}$  and  $\text{Pt}_{\text{DAP}}$  electrodes. The peak potentials for methanol oxidation on the stabilized carbon supported catalysts shift to more negative potentials as compared to the  $\text{Pt}_{\text{Black}}$  (Table 2), indicating that even though the stabilized Pt catalysts displayed higher particle size than that showed for  $\text{Pt}_{\text{Black}}$  a comparable catalytic activity ( $\text{Pt}_{\text{TBA}}$  and  $\text{Pt}_{\text{DAP}}$ ) can be obtained; then, the choice of a suitable amino stabilizer can enhance the per-

formance of these Pt catalysts on MOR. The fact of that the peak current density for  $\text{Pt}_{\text{TBA}}$  ( $11.97 \text{ mA cm}^{-2}$ ) has been comparable to that previously reported by other authors[55, 56] corroborates the assumption of a good catalytic activity when the Pt nanoparticles are stabilized with TBA and it is also in good agreement with studies using nanostructure electrodes on MOR[55, 56]. Small differences are also observed in the onset potential of methanol oxidation reaction (~350 mV); which indicates that all catalysts involved the formation of platinum hydroxide compounds and consequently, it is obvious that these hydroxide species are involved in the mediation of the methanol oxidation reaction, favoring the reaction even when the different amino groups are present [57].

In summary, the  $\text{Pt}_{\text{TBA}}$  nanoparticles have significant current densities and are comparable to the behavior of commercial catalysts. The current density peak, appearing at different potentials, increases in the following order  $\text{Pt}_{\text{Black}} \equiv \text{Pt}_{\text{TBA}} > \text{Pt}_{\text{DAP}} > \text{Pt}_{\text{AA}}$ . During the backward sweep process, an anodic peak is detected at around 600 mV (SCE). The appearance of the prominent symmetry for  $\text{Pt}_{\text{TBA}}$ ,  $\text{Pt}_{\text{DAP}}$  and  $\text{Pt}_{\text{Black}}$  at this potential resembles the methanol electro-oxidation while  $\text{Pt}_{\text{DAP}}$  is far of a symmetric shape. In the backward scan, this peak has been attributed to the removal of incompletely oxidized carbonaceous species formed in the forward scan in an electrolyte [58, 59]. The results can be explained as follows: The particle size distribution was fairly narrow, as show by the TEM measurements and the histograms, with deviations of about 10-20% in the different systems. The larger sizes of the AA and TBA could be attributable to the larger particles initially formed in the reaction, which causes that after the phase transfer occurs an agglomeration. Indeed, it is also necessary to consider that amino compounds function as steric ("ligand") stabilizer for metal nanoparticles [60, 61], where the size and dispersibility of obtained Pt particles can be controlled by the chain length of alkylamines or amine group. Theoretical reports have shown that the different association behavior of the primary, secondary, and tertiary amines upon identical experimental conditions depends on the steric effect which is quite important during the stabilization of metallic particles [62]. Primary amines exhibit a high tendency to form large complexes and in specific conditions favors to formation of high-order clusters than their counterparts. Then, the tendency to produce clusters from solution in the electrospray source may serve as an indication for a more general structural competence of specific building blocks to associate. Their different tendency to form aggregates must therefore result from the differences in their sterical shapes rather than different acid-base interactions.

In this work, it is also interesting to note that the CV curves have their own characteristics. For instance,  $\text{Pt}_{\text{DAP}}$  displayed shoulder-like waves at 600 mV in the anodic direction, while  $\text{Pt}_{\text{TBA}}$  and  $\text{Pt}_{\text{AA}}$  only exhibit a single broad peak during methanol oxidation, which is similar to the commercial Pt nanoparticles, although in the last case, it displayed a relatively broad and large peak. The observed shoulder has recently been explained by assuming that CO reacts at the low potential steps [63], which acts as a catalysts poison. In this case, the continuous surface reaction between the CO and OH adsorbed species [64] from water decomposition causes the formation of carbon dioxide according to the following pathway [65-69]:

Table 2. Onset of methanol oxidation reaction, potential and current peak in the forward scan.

Electrode	$E_{\text{p}}(\text{mV})$	$i_{\text{p}} (\text{mA cm}^{-2})$	$E_i(\text{mV})$
$\text{Pt}_{\text{TBA}}$	891	11.97	334
$\text{Pt}_{\text{DAP}}$	893	8.32	365
$\text{Pt}_{\text{DAP}}$	822	6.4	396
$\text{Pt}_{\text{Black}}$	934	13.1	352

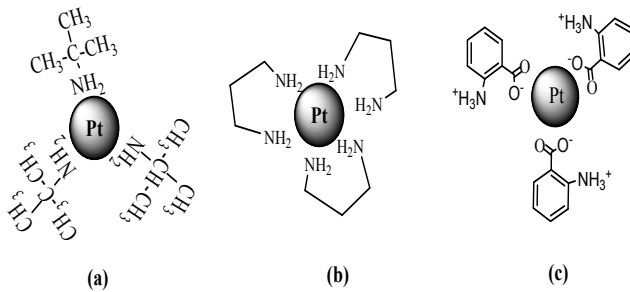
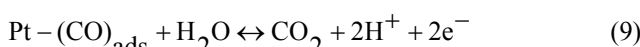
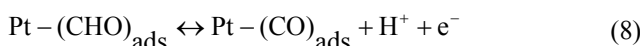
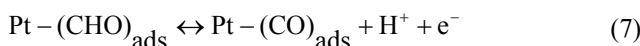
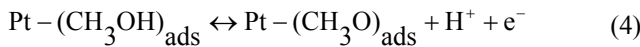


Figure 6. Schematic representation of stabilized Pt nanoparticles:  
(a)  $\text{Pt}_{\text{TBA}}$ , (b)  $\text{Pt}_{\text{DAP}}$  and (c)  $\text{Pt}_{\text{AA}}$ .



Then, the low activities obtained by using AA ligand in comparison with those obtained with  $\text{Pt}_{\text{TBA}}$ ,  $\text{Pt}_{\text{black}}$  and  $\text{Pt}_{\text{DAP}}$  can be explained as follows: for methanol oxidation, at least three adjacent Pt sites are necessary to activate the chemisorptions of methanol. The probability of obtaining the three adjacent Pt sites on the stabilized nanostructures with AA seems to be lower than that observed for their counterparts. The three stabilizers can be considered as weak coordination ligands that allow the access to the surface platinum nanoparticles (Figure 6). However, previous works related to alkylamine ligands used as stabilizers in metallic particles have shown that the amine group at the surface of the metallic nanoparticles evidenced certain mobility that can lead to a temporary lack of amine on the platinum nanoparticle surfaces [4]. This temporary amine lack can be more easily reached in this case with TBA than that expected for DAP, which exhibited the lowest particle size. The presence of two amine groups contained in DAP can cause a better stabilization to platinum nanoparticles because of the coordination, but at the same time, it leads to less structures and more active sites. In the case of AA, it is expected to interact with the metal through the two oxygen atoms [46], hence AA could perhaps be more susceptible to leave exposed larger Pt surface areas, and thus form bigger aggregates than with TBA or DAP due to the

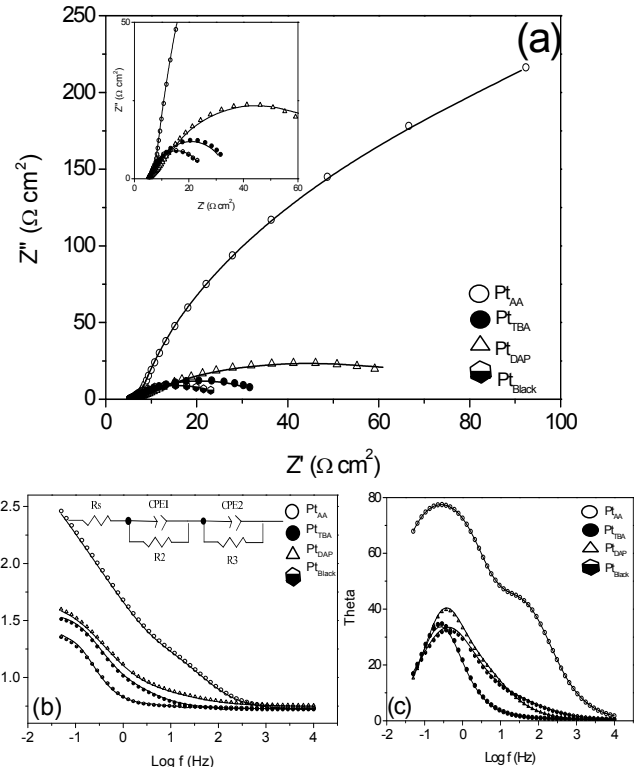


Figure 7. Electrochemical impedance spectra of stabilized Pt catalysts and commercial Pt black for the forward sweep at 400 mV over methanol oxidation reaction. Lines are the fits to the selected equivalent circuit.

lower coordination ability of oxygen to platinum with respect to the nitrogen atoms, but such susceptibility is affecting their stability to lead denser structures and less active sites.

The previous results demonstrate several important points. Firstly, the use of a suitable ligand during the synthesis of Pt nanostructures could modify the catalytic activity on MOR, ORR [37] or HER [46] because of the dispersion of particles provided by the coordination ligands on the metallic surface; secondly, they show that the molecular layers do not necessarily act as blocking layers for electron transport, but modify the exposed surface area, which can facilitate the electron-transfer reaction to redox species in solution; finally, it has been found that stabilized Pt nanoparticles using TBA or even DAP exhibit an interesting electrocatalytic activity, and can facilitate the MOR.

### 3.4. Electrochemical impedance spectroscopy analysis

It has been proposed by different authors that impedance spectroscopy is a direct method to study the electrochemical processes involved in MOR [70, 71] and from these ones, the most common way to present the Nyquist and Bode diagrams as a function of electrode potential, which have shown special qualitative features depending on the potential [72]. For this reason, the electrochemi-

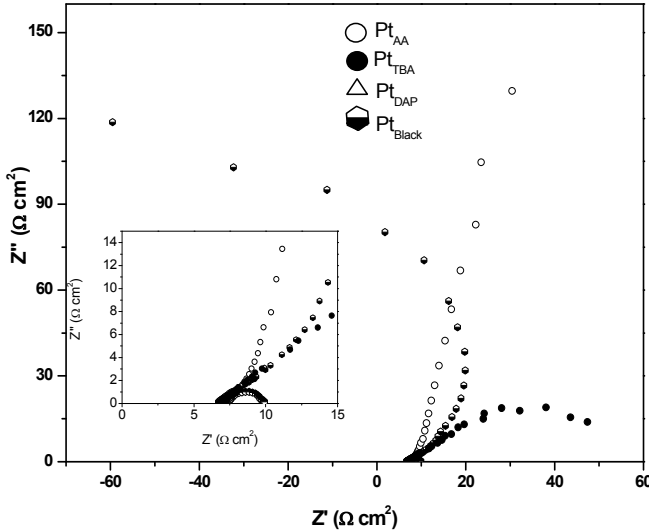


Figure 8. Nyquist plots for methanol oxidation on stabilized Pt nanostructures prepared by organometallic approach for the forward sweep at 900 mV in 0.5M H<sub>2</sub>SO<sub>4</sub>+ 0.1 M CH<sub>3</sub>OH.

cal studies were commented with EIS analysis to deeply investigate the catalyst behavior using two different electrode potentials (400 and 900 mV). Nyquist and Bode spectra of supported Pt-stabilized catalysts in 0.5M H<sub>2</sub>SO<sub>4</sub>+ 0.1 M CH<sub>3</sub>OH at 400 mV are shown in Figure 7a-c. These values were fitted by using the inset equivalent circuit shown in Figure 7b. In the proposed circuit, R<sub>s</sub> is the solution resistance, R<sub>2</sub> can be attributed to the CO<sub>ads</sub> oxidation reaction resistance in parallel with a constant phase element (CPE<sub>1</sub>). The most accepted interpretation of the considered EIS data is that additional adsorbed species are present on the Pt surface such as CO, water, OH or oxides, but it is also agreed that the turnover rate of all but one intermediate is fast, and in such a case, the adsorbed compounds behave as a resistance[73-75]. R<sub>3</sub> is proposed as the charge-transfer resistance due to the methanol oxidation kinetics in parallel with the constant phase element (CPE<sub>2</sub>) associated with the capacitance of the double layer. The impedance of the CPE has the form of  $Z_{CPE} = \frac{1}{Q(j\omega)^f}$  and was used to simulate the depression of the semicircle in the complex plane; where Q is the capacitance relative to the average double layer parameter  $Q = C_{dl}^{\phi}(R_s^{-1} + R_{ct}^{-1})^{1-\phi}$ ; f, is the CPE exponent 0  $\leq$  f  $\leq$  1. The most widely accepted explanation of the presence of CPE behavior and depressed semicircles

on solid electrodes is microscopic roughness, causing a coupling of the solution resistance and the double-layer capacitance [71]. Detailed fitting results are listed in Table 3. After stabilization tests, the resistance solution (R<sub>s</sub>) remains almost constant during electrocatalytic evaluation; commercial nanoparticles (Pt<sub>Black</sub>) showed lower solution resistance (4.86 W cm<sup>2</sup>) as compared with its counterparts. Even though, the solution resistance is due to the movement of ionic species affected by concentration and temperature, (i.e. it is a bulk property), and independent of the interfacial properties of the electrode, it is reasonable to expect small differences because real electrochemical cells do not have uniform current distributions through a definite electrolyte area [76]. The CO<sub>ads</sub> resistance associated with interfacial properties of the Pt-stabilized nanoparticles and the corresponding resistances to charge transfer resistance showed important differences depending upon amine group used during catalyst preparation; which varies up to ~30 times in magnitude as compared with that shown by Pt<sub>Black</sub>. It is well known that the magnitude of the semicircle is related with the activity of the electro-oxidation methanol kinetics [70-72]. The extent of the decrease in resistance indicates the increasing driving force for the methanol oxidation process. Then, the fitted parameters shown in Table 3 clearly indicate that the TBA used as stabilizer has a lower resistance than that shown by DAP and AA. These impedance results are also in good agreement with cyclic voltammetry and prove the assumption of the weak interaction of two oxygen atoms contained in AA at the surface of Pt nanoparticles.

As electrode potential increases up to 900 mV, the characteristic EIS behavior begins to appear (Figure 7). In the case of Pt<sub>Black</sub> and Pt<sub>AA</sub>, the diameter of the primary semicircle decreases considerably, indicating a process active by potential, even the charge transfer resistance tends to decrease. On the other hand, in the Pt<sub>DAP</sub> and Pt<sub>TBA</sub> electrodes, the semicircle began to increase and flips over the second quadrant of the complex plane. The shape of Nyquist plots matches the well-known different stages that can occur with the potential electrode during MOR with the increase of the potential electrode [70, 71]. Due to the fact that significant errors can be obtained when the data are fitted in the second quadrant in the Nyquist plots because of the reciprocal of small numbers crossing through zero and some slight change in this region at the different regions can be magnified, it was prudently considered not to propose an equivalent circuit at 900 mV. However, it is clear that the potential dependence of the involved resistances and the rate determining step are strongly modifying the impedance response depending on the functional group present as stabilizer. Finally, impedance spectroscopy of electron oxidation of methanol on stabilized platinum nanoparticles indicates that although the ligands are modifying kinetically the MOR, this modification is only due to the stabilization of nanostructures leaving a higher exposed surface area. The adsorption strength of oxygenated species on Pt increases with decreasing particle sizes [57, 77], thus limiting the adsorption of methanol species and in consequence the turnover of all other intermediates is too fast to be detected.

#### 4. CONCLUSIONS

The effect of amino groups used as stabilizers (ligands) to obtain Pt electrodes by using an organometallic approach was evaluated in MOR. Diffuse reflectance spectra confirm the presence of amine ligands near the surface of the metallic particles after the purifica-

Table 3. Fitting results of EIS measurements at 400 mV.

Parameters	Pt	Pt <sub>AA</sub>	Pt <sub>DAP</sub>	Pt <sub>TBA</sub>
R <sub>s</sub> (Ω cm <sup>2</sup> )	4.86	5.65	5.64	5.24
R <sub>2</sub> (Ω cm <sup>2</sup> )	3.74	18.10	9.46	3.54
Y <sub>O1</sub> (Ω <sup>-1</sup> sec <sup>n</sup> )	0.34E-1	4.50E-3	6.91E-4	0.10E-1
n <sub>1</sub>	0.79	0.66	0.59	0.72
R <sub>3</sub> (Ω cm <sup>2</sup> )	19.44	603	67.6	26.8
Y <sub>O2</sub> (Ω <sup>-1</sup> sec <sup>n</sup> )	0.5688E-1	0.141E-1	0.5597E-2	0.310E-1
n <sub>2</sub>	0.94	0.94	0.77	0.94

tion step. TEM studies demonstrated that the contributions of the ligands cause small discrepancies in the interatomic distances as a result of the interaction between the skeleton and the functional groups. The formation of uniform and well-shaped particles can be accounted for as a consequence of balance between stabilization and crystal growth in the solvent. Pt nanostructures using 1,3-DAP as stabilizer seems to be better (polydisperse in shape and size) than the others obtained with TBA and AA ("sponge-like" agglomerates). The proposed Pt nanoparticles with amine ligands are stable in solution and could be easily precipitated out of solution as a powder and re-dispersed in different organic solvents without significant variation in the particle size to prepare electrode materials. The as-prepared electrodes displayed a good stability after 50 potential cycles which can be of great importance for industrial applications. The Pt<sub>TBA</sub> electrode shows higher electrocatalytic activity, higher current density and lower transfer resistance as compared with those shown by the Pt<sub>DAP</sub> and Pt<sub>AA</sub>. The electrochemical performance of the as-prepared materials showed the importance of the stabilizer nature and steric effect, allowing the access to the active sites of the nanostructures and contributing to the electron donation effect from the nitrogen atom of the amino group. Finally, the significance of this work is that the information concerning the shape, size, surface state and stability of noble metal nanostructures contributes to the enhancement of the electrochemical properties for a particular reaction, originating an important outcome for developing better electrocatalysts by means of a suitable ligand.

## 5. ACKNOWLEDGEMENTS

The authors wish to acknowledge the financial support provided by CONACYT through the 59921 and 61354 projects, SIP-IPN 2010-0087, 2010-0062 and SNI-CONACYT. The authors would like to thank Ms. Cynthia Carolina Villanueva-Alvarado for her technical support.

## REFERENCES

- [1] D. Wostek-Wojciechowska, J.K. Jeszka , C. Amiens, B. Chaudret, P. Lecante, *J. Colloid Interface Sci.*, 287, 107 (2005).
- [2] F. Dassenoy, K. Philippot, T. Ould-Ely, C. Amiens, P. Lecante, E. Snoeck, A. Mosset, M.J. Casanove, B. Chaudret, *New J. Chem.*, 22, 703 (1998).
- [3] C. Pan, K. Pelzer, K. Philippot, B. Chaudret, F. Dassenoy, P. Lecante, M.J. Casanove, *J. Am. Chem. Soc.*, 123, 7584 (2001).
- [4] E. Ramirez, L. Eradès, K. Philippot, P. Lecante, B. Chaudret, *J. Adv. Funct. Mater.*, 13, 2219 (2007).
- [5] O. Margeat, F. Dumestre, C. Amiens, B. Chaudret, P. Lecante, M. Respaud, *Prog. Solid State Chem.*, 33, 71 (2005).
- [6] S. Gómez, L. Eradès, K. Philippot, B. Chaudret, V. Collière, O. Balmes, J.O. Bovin, *Chem. Commun.*, 1474 (2001).
- [7] F. Dumestre, C. Amiens, B. Chaudret, M.C. Fromen, M.J. Casanove, P. Renaud, P. Zurcher, *Mater. Res. Soc. Symp. Proc.*, 735, 165 (2003).
- [8] A.B.R. Mayer, J.E. Mark, R.E. Morris, *Polym. J.*, 30, 197 (1998).
- [9] W. Yu, M. Liu, H. Liu, X. Ma, Z. Liu, *J. Colloid Interface Sci.*, 208, 439 (1998).
- [10]J. Garcia-Martinez, R.W.J. Scott, R.M. Crooks, *J. Am. Chem. Soc.*, 125, 11190 (2003).
- [11]M.J. Hostetler, J.E. Wingrate, C.J. Zhong, J.E. Harris, R.W. Vachet, M.R. Clark, J.D. Londono, M.D. Green, J.J. Stokes, G.D. Wignall, G.L. Glish, M.D. Porter, N.D. Evans, C.B. Murray, *Langmuir*, 14, 17 (1998).
- [12]G. Viau, R. Brayner, L. Poul, N. Chakroune, L.E.F. Fievet-Vincent, F. Fievet-Vincent, *Chem. Mater.*, 15, 486 (2003).
- [13]C. Pan, K. Pelzer, K. Philippot, B. Chaudret, F. Dassenoy, P. Lecante, M.J. Casanove, *J. Am. Chem. Soc.*, 123, 7584 (2001).
- [14]F. Tian, K.J. Klabunde, *New J. Chem.*, 22, 1275 (1998).
- [15]S.W. Kim, J. Park, Y. Jang, Y. Chung, S. Hwang, T. Hyeon, *Nano Lett.*, 3, 1289 (2003).
- [16]G. Schmid, V. Maihack, F. Lantermann, S. Peschel, *J. Chem. Soc., Dalton Trans.*, 589 (1996).
- [17]M. Tamura, H. Fujihara, *J. Am. Chem. Soc.*, 125, 15742 (2003).
- [18]M.N. Vargaftik, V.P. Zagorodnikov, I.P. Stolarov, I.I. Moiseev, D.I. Kochubey, V.A. Likhobov, A.L. Chuvilin, K.I. Zamaraev, *J. Mol. Catal. A: Chem.*, 53, 315 (1989).
- [19]N. Toshima, Y. Shiraishi, T. Teranishi, M. Miyake, T. Tominaga, H. Watanabe, W. Brijoux, H. Bönnemann, G. Schmid, *Appl. Organomet. Chem.*, 15, 178 (2001).
- [20]B.J. Hornstein, R.G. Finke, *Chem. Mater.*, 15, 899 (2003).
- [21]R.G. Finke, S. Özkar, *Coord. Chem. Rev.*, 248, 135 (2003).
- [22]M. Moreno-Manas, R. Pleixats, S. Villarroya, *Organometallics*, 20, 4524 (2001).
- [23]M. Moreno-Manas, R. Pleixats, S. Villarroya, *Chem. Commun.*, 60 (2002).
- [24]C. Amiens, D. de Caro, B. Chaudret, J.S. Bradley, R. Mazel, C. Roucau, *J. Am. Chem. Soc.*, 115, 11638 (1993).
- [25]A. Rodriguez, C. Amiens, B. Chaudret, M.J. Casanove, P. Lecante, J.S. Bradley, *Chem. Mater.*, 8, 1978 (1996).
- [26]A. Duteil, R. Queau, B. Chaudret, R. Mazel, C. Roucau, J.S. Bradley, *Chem. Mater.*, 5, 341 (1993).
- [27]C. Amiens, T.O. Ely, B. Chaudret, E. Snoeck, M. Verelst, M. Respaud, J.M. Broto, *Chem. Mater.*, 11, 526 (1999).
- [28]J. Osuna, D. de Caro, C. Amiens, B. Chaudret, E. Snoeck, M. Respaud, J.M. Broto, A. Fert, *J. Phys. Chem. B*, 100, 14571 (1996).
- [29]F. Dassenoy, M.J. Casanove, P. Lecante, M. Verelst, E. Snoeck, A. Mosset, T.O. Ely, C. Amiens, B. Chaudret, *J. Chem. Phys.*, 112, 8137 (2000).
- [30]J.S. Bradley, E.W. Hill, S. Behal, C. Klein, B. Chaudret, A. Duteil, *Chem. Mater.*, 4, 1234 (1992).
- [31]X. Ren, P. Zelenay, A. Thomas, J. Davey, S. Gottesfeld, *J. Power Sources*, 86, 111 (2000).
- [32]D. Kim, E.A. Cho, S.A. Hong, I.H. Oh, H.Y. Ha, *J. Power Sources*, 130, 172 (2004).
- [33]B.D. McNicol, *J. Electroanal. Chem.*, 118, 71 (1981).
- [34]C. Susut, T.D. Nguyen, G.B. Chapman, Y.Y. Tong, *Electrochim. Acta*, 53, 6135 (2008).
- [35]G. Schmid, M. Baümle, M. Geerkens, I. Heim, C. Osemann, T.

- Sawitowski, Chem. Soc. Rev., 28, 179 (1999).
- [36]M.A. El-Sayed, Acc. Chem. Res., 34, 257 (2001).
- [37]E. Ramírez-Meneses, M.A. Domínguez-Crespo, V. Montiel-Palma, V.H. Chávez-Herrera, E. Gómez, G. Hernández-Tapia, J. Alloys Compd., 483, 573 (2009).
- [38]J. Perez, E.R. Gonzalez, E.A. Ticianelli, Electrochim. Acta, 44, 1329 (1998).
- [39]K. Moseley, P.M. Maitlis, J. Chem. Soc., Chem. Commun., 982 (1971).
- [40]S. Nath, S. Jana, M. Pradhan, T. Pal, J. Colloid Interface Sci., 341, 333 (2010).
- [41]T. Horikoshi, M. Itoh, M. Kurihara, K. Kubo, H. Nishihara, J. Electroanal. Chem., 473, 113 (1999).
- [42]M. Yamada, T. Tadera, K. Kubo, H. Nishihara, J. Phys. Chem. B, 107, 3703 (2003).
- [43]L.E. Euliss, S.G. Grancharov, S.O'Brien, T.J. Deming, G.D. Stucky, C.B. Murray, G.A. Held, Nano Lett., 3, 1489 (2003).
- [44]D. Portet, B. Denizot, E. Rump, J.J. Lejeune, P.J. Jallet, Colloid Interface Sci., 238, 37 (2001).
- [45]D.I. Gittins, F. Caruso, Chem. Phys. Chem., 3, 110 (2002).
- [46]M.A. Domínguez-Crespo, E. Ramírez-Meneses, V. Montiel-Palma, A.M. Torres-Huerta, H. Dorantes-Rosales, Int. J. Hydrogen Energy, 34, 1664 (2009).
- [47]E. Ramírez, S. Jansat, K. Philippot, P. Lecante, Monserrat Gómez, A. M. Masdeu-Bultó, B. Chaudret, J. Organomet. Chem., 689, 4601 (2004).
- [48]R. Czerw, M. Terrones, J.C. Charlier, X. Blase, B. Foley, R. Kamalakaran, N. Grobert, H. Terrones, D. Tekleab, P.M. Ajayan, W. Blau, M. Ruhle, D.R. Carroll, Nano Lett., 1, 457 (2001).
- [49]L. Yang, J. Chen, X. Wei, B. Liu, Y. Kuang, Electrochim. Acta, 53, 777 (2007).
- [50]Z. Shen, Z. Zhao, H. Peng, M. Nygren, Nature, 417, 266 (2002).
- [51]X. Peng, J. Wickham, A.P. Alivisatos, J. Am. Chem. Soc., 120, 5343 (1998).
- [52]Chi-Chang Hu, Kweun-Yo Liu, Electrochim. Acta, 44, 2727 (1999).
- [53]Yi-Fu Yang, G. Denuault, J. Electroanal. Chem., 443, 273 (1998).
- [54]F. Villiard, G. Jerkiewicz, Can. J. Chem., 75, 1656 (1997).
- [55]A. Kelaidopoulou, E. Abelidou, G. Kokkinidis, J. Appl. Electrochem., 29, 1255 (1999).
- [56]H. Laborde, J.M. LeÂger, C. Lamy, J. Appl. Electrochem., 24, 219 (1994).
- [57]T. Frelink, W. Visscher, J.A.R. Van Veen, J. Electroanal. Chem., 382, 65 (1995).
- [58]R. Manohara, J.B. Goodenough, J. Mater. Chem., 2, 875 (1992).
- [59]D.J. Guo, S.K. Cui, J. Solid State Electrochem., 12, 1393 (2008).
- [60]B.S. Ong, Y. Wu, P. Liu, S. Gardner, J. Am. Chem. Soc., 126, 3378 (2004).
- [61]M. Yamamoto, M. Nakamoto, J. Mater. Chem., 13, 2064 (2003).
- [62]C. Denekamp, E. Egbaria, J. Am. Soc. Mass. Spectrom., 15, 356 (2004).
- [63]S.C.S. Lai, N.P. Lebedeva, T.H.M. Housmans, M.T.M. Koper, Top. Catal., 46, 320 (2007).
- [64]H. Razmi, E. Habibi, H. Heidari, Electrochim. Acta, 53, 8178 (2008).
- [65]M.H. Pournaghi-Azar, B. Habibi-A, J. Electroanal. Chem., 580, 23 (2005).
- [66]L. Niu, Q. Li, F. Wei, S. Wu, P. Liu, X. Cao, J. Electroanal. Chem., 578, 331 (2005).
- [67]F. Vigier, F. Gloaguen, J.M. Léger, C. Lamy, Electrochim. Acta, 46, 4331 (2001).
- [68]P. Ross, N. Markovic, Cat. Tech., 4, 110 (2000).
- [69]M.H. Pournaghi-Azar, B. Habibi, J. Electroanal. Chem., 601, 53 (2007).
- [70]S. Loka Subramanyam, L. Tzu Dai, T. Yin-wen, C. Jium Ming, H. Bing Joe, J. Power Sources, 139, 44 (2005).
- [71]R.E. Melnick, G.T.R. Palmore, J. Phys. Chem. B, 105, 1012 (2001).
- [72]F. Seland, R. Tunold, D.A. Harrington, Electrochim. Acta, 51, 3827 (2006).
- [73]J.T. Müller, P.M. Urban, W.F. Hölderich, J. Power Sources, 84, 157 (1999).
- [74]J. Otomo, X. Li, T. Kobayashi, C. Wen, H. Nagamoto, H. Takahashi, J. Electroanal. Chem., 573, 99 (2004).
- [75]R.E. Melnick, G.T.R. Palmore, J. Phys. Chem. B, 105, 1012 (2001).
- [76]A.J. Bard, G. Inzelt, F. Sholz, Electrochemical Dictionary, Springer, Verlag Berlin Heidelberg, 2008, pp. 581.
- [77]F. Gloaguen, J.M. Léger, C. Lamy, J. Appl. Electrochem., 27, 1052 (1997).